Structural stability of one-dimensional long-period structures in the $TiAl_3$ compound

2002 J. Phys.: Condens. Matter 14 6713

(http://iopscience.iop.org/0953-8984/14/26/311)

INSTITUTE OF PHYSICS PUBLISHING JOURNAL OF PHYSICS: CONDENSED MATTER

J. Phys.: Condens. Matter **14** (2002) 6713–6727 PII: S0953-8984(02)31898-8

Structural stability of one-dimensional long-period structures in the $TiAl_3$ compound

C Colinet[1,3] and A Pasturel[2]

[1] Laboratoire de Thermodynamique et Physico-Chimie Métallurgiques, CNRS/INPG/UJF, ENSEEG, BP 75, 38402 Saint Martin d'Hères, France
[2] Laboratoire de Physique et Modélisation des Milieux Condensés, Maison des Magistères, CNRS, BP 166, 38042 Grenoble Cedex 09, France

E-mail: ccolinet@ltpcm.inpg.fr

Received 14 December 2001, in final form 2 April 2002
Published 21 June 2002
Online at stacks.iop.org/JPhysCM/14/6713

Abstract
The cohesive energies of $L1_2$, $D0_{22}$, $D0_{23}$ and selected one-dimensional long-period structures (1D-LPSs) based on the $L1_2$ structure in the Ti–Al system for the $TiAl_3$ composition have been obtained by *ab initio* calculations using the Vienna *ab initio* simulation package. The 1D-LPSs are described within an Ising-like antiphase boundary (APB) model and we take into account both cell-external and cell-internal relaxations in the determination of their structural stability. Thus, the values of the APB energies are obtained in the ideal, distorted and fully relaxed structures. The results show that it is necessary to consider long-range interactions in order to obtain reliable values of the APB energies. We also relate these so-obtained APB energies to the energetic value of an isolated APB.

1. Introduction

The study of early-transition-metal (TM) trialuminides, $TMAl_3$, is of both technological and fundamental interest. The $TMAl_3$ compounds are attractive as potential structural materials for use in high-temperature environments or as thermally stable precipitates for developing so-called 'super alumalloys'.

Furthermore, it is important to emphasize that the crystal structure of these TM trialuminides depends on the location of the early TM in the periodic classification. The stable cubic $L1_2$ structure occurs for $ScAl_3$ only at room temperature and tetragonal $D0_{22}$ and $D0_{23}$ structures appear as the number of d electrons of the TM element increases. It is tempting therefore to relate the ordering tendency of such TM compounds to their electron to atom ratio [1]. Another way to analyse this ordering tendency is to note that the tetragonal $D0_{22}$ and $D0_{23}$ structures are derived from the cubic $L1_2$ by inserting (001) antiphase boundaries (APBs)

[3] Author to whom any correspondence should be addressed.

0953-8984/02/266713+15$30.00

every fcc cube along the (001) axis for the $D0_{22}$ structure and every two fcc cubes for the $D0_{23}$ one. For instance, if the interactions between the APBs are neglected, the (001) APB energy may be deduced directly from the energy difference between $L1_2$ and $D0_{22}$ structures:

$$E_{APB} = E_{D0_{22}} - E_{L1_2}. \quad (1)$$

Considering the energy difference from $L1_2$ of the $D0_{23}$ structure, one obtains in this simple model

$$E_{APB} = 2(E_{D0_{23}} - E_{L1_2}). \quad (2)$$

In relations (1) and (2), the APB energy is defined per atom if the energies of $L1_2$, $D0_{22}$ and $D0_{23}$ are expressed per atom.

Another interest in using the APB as an energetic criterion for phase stability is to relate the mechanical properties of these compounds to their structures since the energies involved in the formation of APBs are instrumental in most theories of the yield behaviour of ordered intermetallics.

But let us turn back to the study of the structural stability of these arrangements, which is the purpose of the present work. We can say that, if the antiphase energy is small, the system will be degenerated since several arrangements of APBs will compete with the $L1_2$ structure. For some alloys, such a behaviour may lead to the occurrence of one-dimensional long-period structures (1D-LPSs). This kind of chemical ordering has been discovered by Johansson and Linde [2] in the Au–Cu alloys and, more recently, 1D-LPSs have been observed in the Ti–Al system, more particularly for the $Ti_{1+x}Al_{3(1-x)}$ alloys [3, 4].

The understanding of the thermodynamical behaviour of 1D-LPSs represents a great challenge; for the $TiAl_3$ compound, we propose to study the structural stability of series of 1D-LPSs based on the $L1_2$ structure by means of *ab initio* total-energy calculations. We shall show that the simple model leading to equations (1) and (2) is not sufficient to explain the relative stability of such 1D-LPSs and we shall propose discussing the relative stability in the framework of a more sophisticated APB Ising model. More particularly, we shall focus on the influence of both cell-external distortion and cell-internal atomic displacements of the atoms on the interaction parameters of the APB Ising model. Indeed a study performed by Amador *et al* [5] using the full-potential linear muffin tin method has shown how the relaxation effects influence the relative stability of the $L1_2$, $D0_{22}$ and $D0_{23}$ structures in the $TiAl_3$ compound.

The remainder of the paper is as follows. In section 2, the 1D-LPSs based on the $L1_2$ structure are briefly described. In section 3, we present the APB Ising model, which will be used further to analyse the structural stability of the 1D-LPSs. The *ab initio* calculations have been performed using the Vienna *ab initio* simulation package (VASP); the basis of this computer code and the conditions of the calculations are given in section 4. The results of the VASP calculations are presented in section 5. The determination of the interaction parameters of the APB Ising model is presented in section 6. Finally, section 7 summarizes the paper and gives the conclusions.

2. One-dimensional long-period structures

The 1D-LPSs we shall consider in the following are derived from the cubic $L1_2$-type structure A_3B (figure 1). $L1_2$ is ordered on the face-centred cubic lattice and consists, along the (001) cubic direction, of a stacking of pure A planes alternately with mixed AB planes. In the stacking sequence of pure and mixed planes, the translation [001] connects minority atoms in subsequent mixed layers. In contrast, in the $D0_{22}$ structure presented in figure 1 a translation of $c/2$ along the z axis connects minority atoms to majority atoms. The $D0_{22}$ structure may

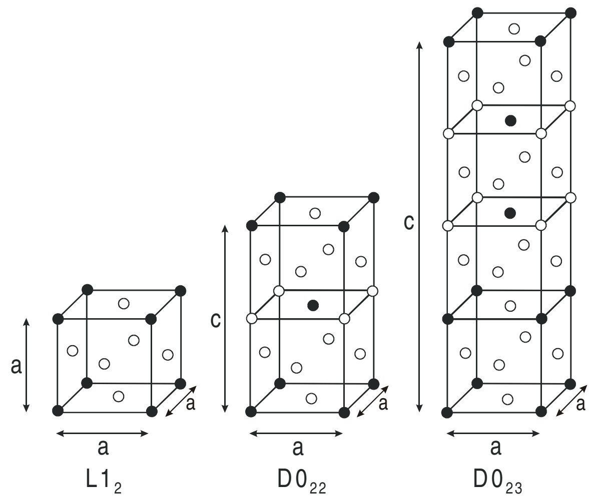

Figure 1. $L1_2$, $D0_{22}$ and $D0_{23}$ 1D-LPSs.

be viewed as a periodic arrangement of (001) APBs in the $L1_2$ structure, the minimal length between the APBs being equal to the height of the $L1_2$ cell. $D0_{22}$ is denoted $1\bar{1}$ in Zdanov's [6] notation or $\langle 1\rangle$ in the notation of Fisher and Selke [7, 8]. $\langle 2\rangle$ 1D-LPS (or $D0_{23}$) consists of a stacking of four $L1_2$ cubes with the same antiphase shift every two cubes. The $\langle M\rangle$ 1D-LPS, M being an integer, consists of a stacking of $2M$ $L1_2$ cubes with the same antiphase shift every M cubes. The 1D-LPSs can be characterized by the average domain size, usually denoted M, which is the ratio of the period and the number of domains or the number of $L1_2$ unit cells divided by the number of APBs in the 1D-LPS unit cell.

Along the z axis, the 1D-LPSs can be seen as Ising chains of spins + and −. Here + and − spins describe the two atomic species A or B in the (001) mixed planes. The $L1_2$ structure corresponds to the ferromagnetic + + + + + + state as the $D0_{22}$ structure corresponds to the antiferromagnetic + − + − + − + − state. An APB with respect to the $L1_2$ structure is like a magnetic domain wall separating two different ferromagnetic domains. Alternatively an APB with respect to the $D0_{22}$ structure is like a magnetic domain wall separating two different antiferromagnetic domains. With this description of the APBs, the $4\bar{4}$ (or $\langle 4\rangle$) 1D-LPS which is + + + + − − − − possesses in its unit cell two APBs with respect to $L1_2$ (++ + +/− − − −/) and six APBs with respect to $D0_{22}$ (+/+/+/+−/−/−/−). Similarly the $2\bar{1}1\bar{2}11$ (or $\langle 21^2\rangle$) which is + + − + − − + − in the spinlike description possesses in its unit cell six APBs with respect to $L1_2$ (+ +/−/+/− −/+/−/) and two APBs with respect to $D0_{22}$ (+/+ − + −/− + −). Let us remark that the $\langle 211\rangle$ 1D-LPS is obtained from $\langle 4\rangle$ by overturning alternate spins. Similarly $\langle 1\rangle$ is obtained from $L1_2$ by overturning alternate spins, and $\langle 21\rangle$ from $\langle 3\rangle$; in this spin change $\langle 2\rangle$ is not modified. More generally, the $\langle 21^j\rangle$ 1D-LPS with $M' = j + 2$ is obtained from the $\langle M\rangle$ 1D-LPS with $M = M'$ by overturning alternate spins.

When one considers 1D-LPSs as based on the $D0_{22}$ structure, it is more convenient to give the period of the superstructure in term of the size M' of the $D0_{22}$ antiphase domain still measured in units of the underlying $L1_2$ structure. M' is related to M by $M' = \frac{M}{M-1}$. $M' = \infty$ for the $D0_{22}$ structure, 1 for $L1_2$, 2 for $D0_{23}$, 3 for $\langle 21\rangle$, 4 for $\langle 211\rangle$ described previously and $j + 2$ for the $\langle 21^j\rangle$ 1D-LPS.

3. Antiphase boundary energy model

As proposed by Bak and Bruinsma [9] and more recently by Rosengaard and Skriver [10], the energy difference of a 1D-LPS from the underlying structure, either $L1_2$ or $D0_{22}$, may be mapped onto a one-dimensional effective Ising Hamiltonian in a field. In this description, the presence of an APB is represented by $\uparrow$ with $\sigma = \frac{1}{2}$ while the absence is represented by $\downarrow$ with $\sigma = -\frac{1}{2}$; the field is given by the APB energy, E_{APB}. The interactions between neighbouring APBs are given by I_n and $H_{n,m}$ for two-and three-body interactions respectively. The energy difference from the reference structure for a given 1D-LPS is

$$E_S - E_{\langle ref\rangle} = \frac{1}{N}\sum_i \left(\sigma_i + \frac{1}{2}\right) E_{APB} + \frac{1}{N}\sum_{j>i} I_{j-i}\left(\sigma_i + \frac{1}{2}\right)\left(\sigma_j + \frac{1}{2}\right) + \frac{1}{N}\sum_{j>i>k} H_{i-k,j-i}\left(\sigma_i + \frac{1}{2}\right)\left(\sigma_j + \frac{1}{2}\right)\left(\sigma_k + \frac{1}{2}\right) \quad (3)$$

where the sums are restricted to nearest-neighbour spins. In the following we shall restrict the three-body interaction to the first term $H_{1,1}$.

When taking the $L1_2$ structure as the reference, the energy difference from $L1_2$ of $\langle M\rangle$ 1D-LPSs, M being an integer, is

$$M(E_{\langle M\rangle} - E_{\langle\infty\rangle}) = E_{APB} + I_M + I_{2M} + \cdots . \quad (4)$$

The APB energy with respect to $L1_2$, E_{APB}, is the limit of $M(E_{\langle M\rangle} - E_{\langle\infty\rangle})$ when $M \to \infty$, but one can expect that expansion (4) converges rapidly. If this is the case, the value of $M(E_{\langle M\rangle} - E_{\langle\infty\rangle})$ becomes constant from some small value of M and the APB energy with respect to the $L1_2$ structure is equal to this constant.

When taking the $D0_{22}$ structure as the reference, energy differences from $D0_{22}$ of the 1D-LPS $\langle 21^j\rangle$, j being an integer, are given by

$$M'(E_{\langle 21^j\rangle} - E_{\langle 1\rangle}) = E'_{APB} + I'_{M'} + I'_{2M'} + \cdots \quad (5)$$

with $M' = j+2$. The APB energy with respect to $D0_{22}$ is the limit of $M'(E_{\langle 21^j\rangle} - E_{\langle 1\rangle})$ when $M' \to \infty$, and if expansion (5) converges rapidly the value of $M'(E_{\langle 21^j\rangle} - E_{\langle 1\rangle})$ becomes constant from some small value of M' and the APB energy with respect to $D0_{22}$, E'_{APB}, is equal to this constant. One can show that the coefficients of the two expansions (4) and (5) are related. The connecting relation between the APB energies is

$$E'_{APB} = -E_{APB} - 2\sum_{M_0-1} I_{M_0-1} - 3H_{1,1} \quad (6)$$

where M_0 is the value of M or M' from which the interaction coefficients can be taken equal to zero.

The purpose of the following is to obtain, from *ab initio* total-energy calculations, the energy differences from $L1_2$ of series of 1D-LPSs $\langle M\rangle$ with M an integer and $\langle 21^j\rangle$. From these energy differences, the APB energy and the interaction parameters will be obtained. Moreover, we shall show that this determination depends on how we compute the energy differences.

4. *Ab initio* calculations

The calculations presented here were performed using the VASP, which has been described elsewhere [11–13]. All calculations were performed in the generalized gradient approximation (GGA) proposed by Perdew and Wang [14]. The electron–ion interaction is described by ultrasoft pseudopotentials which allow the use of a moderate cut-off for the construction of the plane-wave basis even for TMs (222 eV for Ti). For the present calculation of ultrasoft pseudopotentials, the atomic reference configurations were $3p^6\ 4s^1\ 3d^3$ for Ti and $3s^2\ 3p^1$ for Al. For Ti, it is essential to include the 3p states as valence states in order to obtain correct lattice parameters. For Ti, the radii for the calculations of the augmentation functions are $R_{aug,l} = 2.20, 2.00$ and 2.49 au for $l = 2, 1, 0$, respectively; for Al, $R_{aug,l} = 2.36$ for $l = 1$ and 0. Partial core corrections were introduced to enable a proper treatment of the nonlinear dependence of the exchange–correlation functional on the charge density.

For the total-energy calculations of the Al_3Ti compound in the $L1_2$ structure (four atoms in the primitive cell) a $10 \times 10 \times 10$ k-point mesh was chosen. For the 1D-LPS, the same k-point mesh along x and y axes was retained. Along the z axis, the number of k points was reduced as the length of the 1D-LPS increased. We saw in section 3 that the important result of the calculations is the energy difference of a given 1D-LPS from the $L1_2$ structure. To improve the precision of this difference, a $L1_2$ superstructure containing the same number of $L1_2$ unit cells as the considered 1D-LPS has been studied using the same number of k points and its cohesive energy calculated. For each 1D-LPS, the energy difference from $L1_2$ is calculated with respect to the corresponding $L1_2$ superstructure.

5. Results

5.1. Equilibrium structures

From $L1_2$ to $D0_{22}$, and to the other 1D-LPSs, symmetry elements are progressively lost so that relaxation degrees of freedom increase correspondingly. In the $L1_2$ structure, the energy is optimized with respect to the lattice parameter a only. In the $D0_{22}$ structure, the energy optimization is performed with respect to the lattice parameter a and with respect to the c/a ratio (tetragonal distortion of the lattice). Finally, in the $D0_{23}$ and other 1D-LPSs, the lattice parameter a, the c/a ratio (tetragonal distortion of the lattice) and additionally the cell-internal displacements of Ti and Al atoms are optimized.

The lattice parameters obtained in the volume optimization procedure are reported in figures 2 and 3 respectively for the $\langle M\rangle$ and $\langle 21^j\rangle$ 1D-LPSs. The tetragonality reported for one $L1_2$ unit cell is presented in figures 4 and 5 respectively for the $\langle M\rangle$ and $\langle 21^j\rangle$ 1D-LPSs. In the case of ideal structures, the convergence of the lattice parameters of the $\langle M\rangle$ 1D-LPSs to the value obtained in the $L1_2$ structure is fast. Similarly the convergence of the lattice parameters of the $\langle 21^j\rangle$ 1D-LPS to the lattice parameter of the ideal $D0_{22}$ is also fast. In contrast, for the distorted and fully relaxed phases $\langle M\rangle$ and $\langle 21^j\rangle$, the convergence becomes slower and one may observe that the lattice parameters a of the $\langle M\rangle$ 1D-LPSs differ from that of the $L1_2$ structure and that the lattice parameters a of the $\langle 21^j\rangle$ 1D-LPSs differ from that of the $D0_{22}$ structure.

The energy differences from $L1_2$ of all the 1D-LPSs studied in the present work are reported in table 1. In the ideal case, the ground state is $L1_2$. With distortion only, the $D0_{22}$ structure is the ground state. For the fully relaxed phases, the $D0_{23}$ structure is the most stable 1D-LPS; this result is unexpected because experimentally $TiAl_3$ crystallizes in the $D0_{22}$ structure [15]. However, our result is in perfect agreement with that obtained by Amador *et al* [5], who found that $D0_{23}$ is the ground state but by a very small margin. It must be noticed that the displacements of the atoms are small, and it is expected that these displacements will cancel with increasing temperature, explaining why $D0_{22}$ is observed experimentally at room temperature. One must also quote that the $L1_2$ structure has been observed experimentally under particular circumstances (see for example [16]). The values of the energy differences

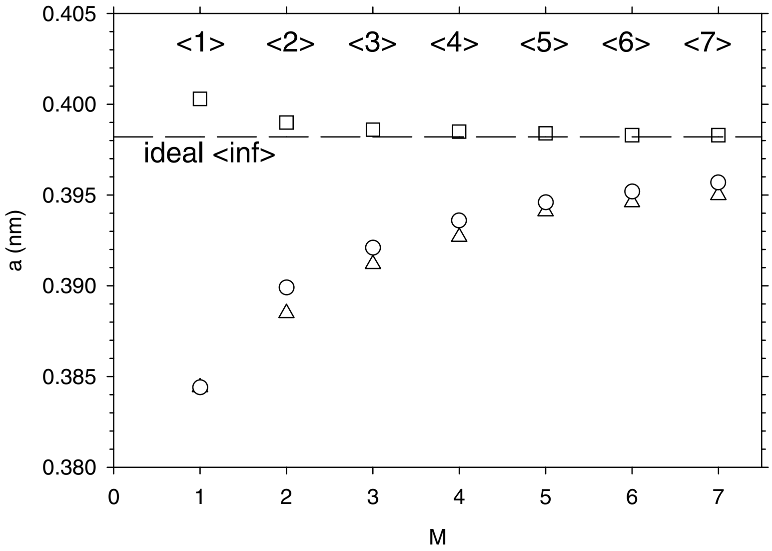

Figure 2. Lattice parameters of the $\langle M \rangle$ 1D-LPSs. □, ideal structures; △, distorted structures; ○, fully relaxed structures.

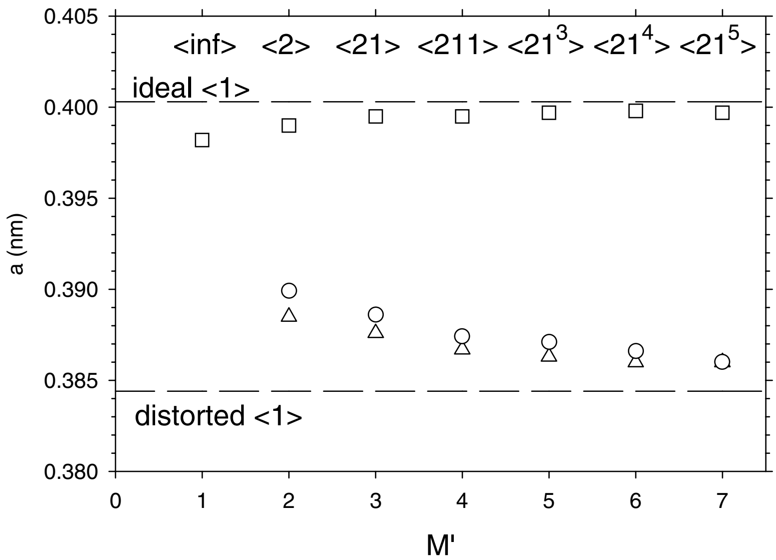

Figure 3. Lattice parameters of the $\langle 21^j \rangle$ 1D-LPSs. □, ideal structures; △, distorted structures; ○, fully relaxed structures.

from $L1_2$ of the series of 1D-LPS $\langle 21^j \rangle$ are very near that of $D0_{22}$ in the distorted case: this explains why 1D-LPSs with one and two bands have been observed experimentally in the Ti–Al system near the $TiAl_3$ composition by Miida *et al* [3] and by Loiseau *et al* [4].

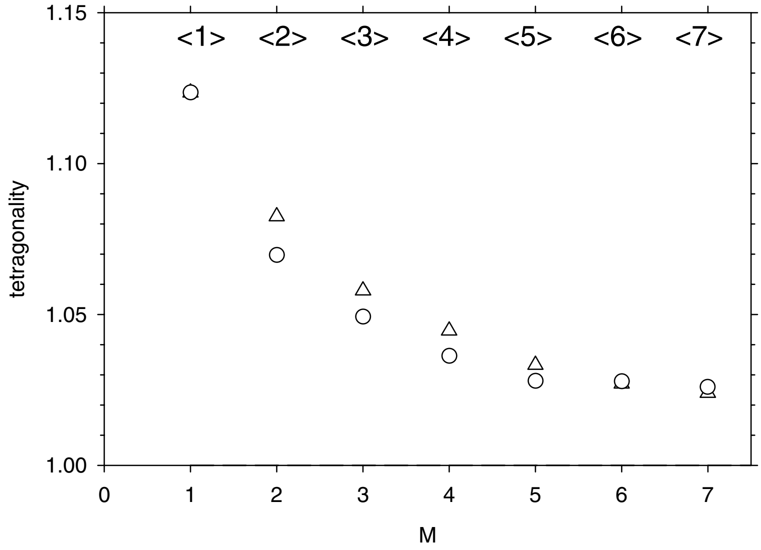

Figure 4. Tetragonality of the $\langle M \rangle$ 1D-LPSs. △, distorted structures; ○, fully relaxed structures.

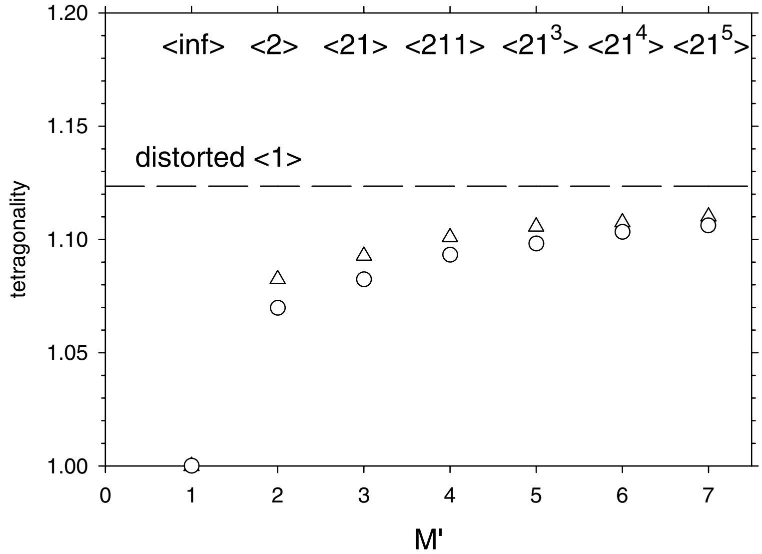

Figure 5. Tetragonality of the $\langle 21^j \rangle$ 1D-LPSs. △, distorted structures, ○, fully relaxed structures.

5.2. Constrained structures

In the previous paragraph, we have seen that the lattice parameters a of the $\langle M \rangle$ 1D-LPSs differ from that of the $L1_2$ structure and that the lattice parameters a of the $\langle 21^j \rangle$ 1D-LPSs differ from that of the $D0_{22}$ structure. Therefore it seems difficult from the previous results to obtain the energy of an isolated APB either in the $L1_2$ or in the $D0_{22}$ structure. Indeed to obtain true information on an isolated APB it is necessary to perform calculations with a constant lattice parameter a, that means with constrained structures. Then, when studying the APBs in the

Table 1. Values of the energy differences from $L1_2$ of equilibrium 1D-LPSs in meV/atom.

1D-LPS	Ideal	Distorted	Fully relaxed
⟨1⟩	46.4	−25.0	−25.0
⟨2⟩	10.8	−20.8	−33.2
⟨3⟩	5.5	−9.6	−21.9
⟨4⟩	3.6	−4.5	−14.8
⟨5⟩	3.5	−1.4	−10.5
⟨6⟩	2.5	0.1	−8.7
⟨7⟩	2.1	0.3	−7.5
⟨21⟩	19.4	−18.9	−31.6
$\langle 21^2 \rangle$	25.8	−20.8	−30.9
$\langle 21^3 \rangle$	29.9	−20.8	−29.2
$\langle 21^4 \rangle$	32.5	−19.6	−28.4
$\langle 21^5 \rangle$	34.9	−19.9	−27.8

Table 2. Values of the energy differences from $L1_2$ of 1D-LPSs constrained to the *a* lattice parameter of the equilibrium $L1_2$ structure in meV/atom.

1D-LPS	Distorted structures along z axis	Fully relaxed structures along z axis
⟨1⟩	33.3	33.3
⟨2⟩	2.0	−16.0
⟨3⟩	1.5	−13.0
⟨4⟩	1.5	−10.7
⟨5⟩	2.0	−8.2
⟨6⟩	1.9	−6.7
⟨7⟩	1.4	−6.3

Table 3. Values of the energy differences from $L1_2$ of $\langle 21^j \rangle$ 1D-LPSs constrained to the *a* lattice parameter of the equilibrium distorted $D0_{22}$ structure in meV/atom.

1D-LPS	Distorted structures along z axis	Fully relaxed structures along z axis
⟨1⟩	−86.2	−86.2
⟨2⟩	−78.6	−89.2
⟨21⟩	−78.1	−89.0
$\langle 21^2 \rangle$	−81.4	−89.2
$\langle 21^3 \rangle$	−81.3	−88.9
$\langle 21^4 \rangle$	−82.6	−88.7
$\langle 21^5 \rangle$	−82.9	−88.4

$L1_2$ structure, the lattice constants in the x and y directions were fixed to the values obtained in the $L1_2$ structure. The c/a ratio along the z axis as well as the displacements in this direction were optimized. The results of such calculations are presented in table 2. Similarly, when studying the APBs in the $D0_{22}$ structure, the lattice constants in the x and y directions were fixed to the values obtained in the $D0_{22}$ structure. The c/a ratio along the z axis as well as the displacements in this direction were optimized. The results of such calculations are presented in table 3.

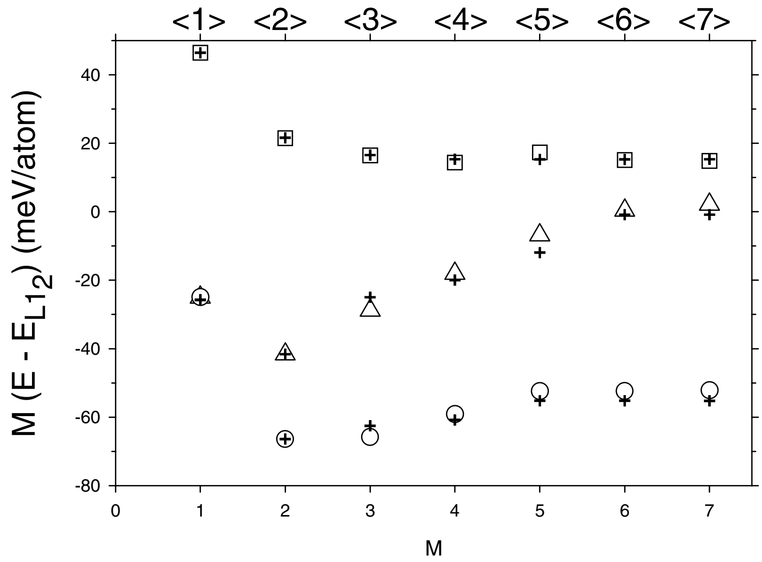

Figure 6. VASP-calculated values of the energy differences from $L1_2$ multiplied by M of $\langle M\rangle$ 1D-LPSs. □, ideal structures; △, distorted structures; ○, fully relaxed structures. The crosshairs represent the values calculated with the APB model using the fitted APB energy and interaction parameters.

6. Application of the APB Ising model

6.1. Equilibrium structures

We shall first consider the equilibrium 1D-LPSs. In these conditions, the parameters of the APB Ising model will give indications of the relative stabilities of the 1D-LPSs. In the following we shall use two methods to derive the values of E_{APB} and E'_{APB}.

6.1.1. Method 1. In the APB model, the value of E_{APB} is theoretically obtained from the value of $M(E_{\langle M\rangle} - E_{\langle\infty\rangle})$ when $M \to \infty$. Similarly the value of E'_{APB} is obtained from $M'(E_{\langle 21^j\rangle} - E_{\langle 1\rangle})$ when $M' \to \infty$. The energy differences from $L1_2$ of $\langle M\rangle$ 1D-LPSs, in the form $M(E_{\langle M\rangle} - E_{\langle\infty\rangle})$, are reported in figure 6. Likewise the $M'(E^j_{\langle 21\rangle} - E_{\langle 1\rangle})$ values for the $\langle 21^j\rangle$ 1D-LPSs are reported in figure 7. In each case, ideal, distorted and fully relaxed structures have been considered. In the ideal case, both $M(E_{\langle M\rangle} - E_{\langle\infty\rangle})$ and $M'(E_{\langle 21^j\rangle} - E_{\langle 1\rangle})$ values converge rapidly and become constant from M or M' equal to four. The value of E_{APB} is obtained as the mean value of $M(E_{\langle M\rangle} - E_{\langle\infty\rangle})$ for $M = 4$–7. Like wise, the value of E'_{APB} is obtained from the mean value of $M'(E_{\langle 21^j\rangle} - E_{\langle 1\rangle})$ for $M' = 4$–7. These values are reported in tables 4 and 5. In the case of distorted 1D-LPSs, the convergence is much slower, and it is only for the phases with M or M' equal to six and seven that both $M(E_{\langle M\rangle} - E_{\langle\infty\rangle})$ and $M'(E_{\langle 21^j\rangle} - E_{\langle 1\rangle})$ are practically constant; the values of E_{APB} and E'_{APB} obtained with the $\langle M\rangle$ phases or with the $\langle 21^j\rangle$ phases are reported in tables 4 and 5. For the fully relaxed phases, the situation is intermediate and one can consider that both $M(E_{\langle M\rangle} - E_{\langle\infty\rangle})$ and $M'(E_{\langle 21^j\rangle} - E_{\langle 1\rangle})$ are constant from M or M' equal to five. The corresponding values of E_{APB} and E'_{APB} are reported in tables 4 and 5. The method used above to obtain the APB energies will be called method 1 in the following.

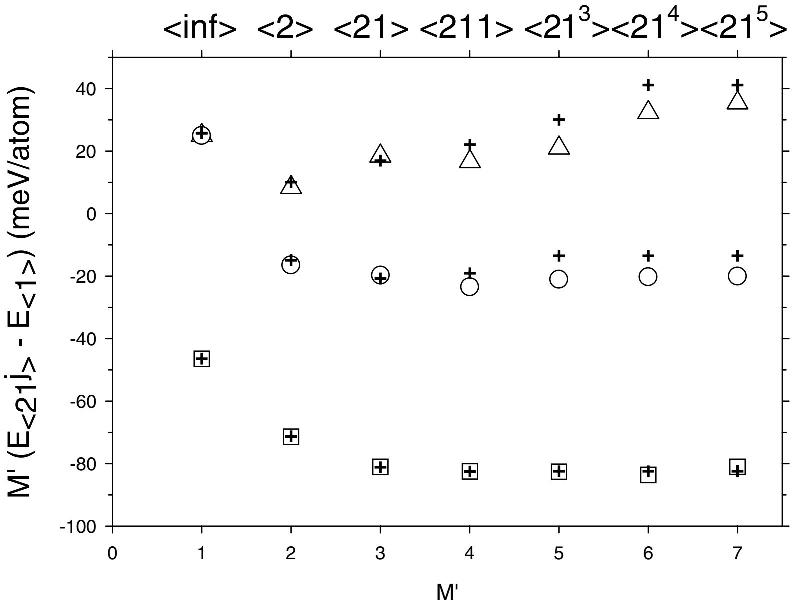

Figure 7. VASP-calculated values of the energy differences from $D0_{22}$ multiplied by M' of $\langle 21^j \rangle$ 1D-LPSs. □, ideal structures; △, distorted structures; ○, fully relaxed structures. The crosshairs represent the values calculated with the APB model using the fitted APB energy and interaction parameters.

Table 4. APB energies with respect to $L1_2$ of the equilibrium 1D-LPSs. The values are given in meV/atom.

	Ideal	Distorted	Fully relaxed
$E_{D0_{22}} - E_{L1_2}$	46	−25	−25
$2(E_{D0_{23}} - E_{L1_2})$	22	−42	−66
E_{APB} (method 1)	15	1	−52
E_{APB} (method 2)	16	−1	−55

Table 5. APB energies with respect to $D0_{22}$ of the equilibrium 1D-LPSs. The values are given in meV/atom.

	Ideal	Distorted	Fully relaxed
$E_{L1_2} - E_{D0_{22}}$	−46	25	25
$2(E_{D0_{23}} - E_{D0_{22}})$	−36	4	−8
E_{APB} (method 1)	−82	34	−20
E_{APB} (method 2)	−83	39	−13

6.1.2. Method 2. However the strategy employed above to obtain the values of E_{APB} and E'_{APB} does not give any information on the interaction parameters between the APBs. To obtain this information, it is necessary to fit the values of the energy differences $E_{\langle M \rangle} - E_{\langle \infty \rangle}$ and $E_{\langle 21^j \rangle} - E_{\langle \infty \rangle}$ in a unique fit because we have shown before that the coefficients of the two expansions (4) and (5) are related. Therefore the values of $E_{\langle M \rangle} - E_{\langle \infty \rangle}$ and $E_{\langle 21^j \rangle} - E_{\langle \infty \rangle}$ have been fitted among expression (3) to obtain the parameters of the APB Ising model. Note that only the first three-spin interaction term has be taken into account, let us say $H_{1,1}$. Various

Table 6. Fitted parameters of the APB Ising model with respect to $L1_2$. The values are given in meV/atom.

	Ideal	Distorted	Fully relaxed
E_{APB}	15.3	−0.9	−55.2
I_1	18.7	41.4	38.2
I_2	6.3	−21.6	−5.6
I_3	1.3	−24.2	−7.3
I_4	0	−19.1	−5.6
I_5	0	−11.1	0
$H_{1,1}$	4.9	9.7	9.7
σ	0.1	0.3	0.2

tests have been performed in which the number of effective pair interaction parameters has been modified. In each case, the standard deviation has been calculated; the goal is to obtain the best fit with the smallest number of parameters. In the ideal case, besides E_{APB} and $H_{1,1}$, it is necessary to introduce three more parameters, let us say I_1, I_2 and I_3. The fit of the values of $E_{\langle M\rangle} - E_{\langle\infty\rangle}$ and $E_{\langle 21^j\rangle} - E_{\langle\infty\rangle}$ is excellent. In the distorted case, seven parameters were necessary to obtain a good fit, E_{APB}, $H_{1,1}$ and I_1–I_5. For the fully relaxed structures, six parameters, E_{APB}, $H_{1,1}$ and I_1–I_4, were necessary to obtain the best fit. As expected, these numbers of parameters are in each case the same as predicted from inspection of figures 6 and 7. All the parameter values as well as the standard deviation are reported in table 6. The calculated parameters are those relative to the APB model with respect to $L1_2$.

The values of $M(E_{\langle M\rangle} - E_{\langle\infty\rangle})$ and $M'(E_{\langle 21^j\rangle} - E_{\langle 1\rangle})$ in the ideal, distorted and fully relaxed cases, recalculated with the three sets of parameters deduced from the fitting procedure, are reported in figures 4(a) and (b). In the ideal case, the representation is excellent. For the distorted and fully relaxed 1D-LPSs, the representation is less satisfying for M or M' equal to six or seven. This point will be explained further. The fitting procedure will be called in the following method 2.

6.1.3. Discussion on the APB model parameters. From inspection of the values of the APB interaction parameters (table 6), one observes that the first-nearest-neighbour interaction parameters are always strongly positive, showing a repulsion between first-nearest-neighbour APBs. The other interaction parameters are either positive and negative.

The values of E_{APB} and E'_{APB} obtained by method 2 are reported in tables 4 and 5 respectively, where they may be compared with the values obtained in method 1. In the ideal case, the difference between the values of E_{APB} and E'_{APB} obtained by method 1 and by method 2 is well within the accuracy of the calculations. In the distorted and fully relaxed cases some differences between the APB energies obtained by method 1 or method 2 appear. Let us recall that in method 1 E_{APB} and E'_{APB} are obtained independently for the $\langle M\rangle$ 1D-LPSs and for the $\langle 21^j\rangle$ ones, while in method 2 the two sets of values are treated in the same model. The observed differences are due to these different treatments. On the other hand, it must be mentioned that the difference is a maximum of 7 meV, which is very small when looking at the precision of the cohesive energy determination and at the fact that the energy differences are multiplied by M or M' in figures 6 and 7 and in tables 4 and 5.

Let us now discuss the values of E_{APB} and E'_{APB} energies. In the ideal case, E_{APB} is positive, showing that APB formation in $L1_2$ is not energetically favoured. In contrast, E'_{APB} is negative, showing that the formation of APBs in the ideal $D0_{22}$ structure is strongly energetically favoured.

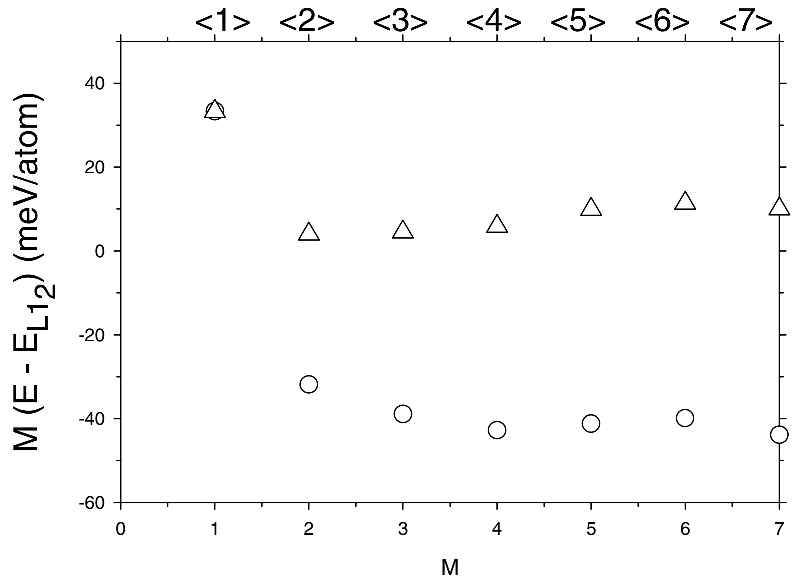

Figure 8. VASP-calculated values of the energy differences from $L1_2$ multiplied by M of $\langle M\rangle$ 1D-LPSs whose lattice parameter, a, has been constrained to that of the $L1_2$ structure. $\triangle$, distorted structures; $\bigcirc$, fully relaxed structures.

In the distorted case, E_{APB} is negative but very small in absolute value. If one looks at the values obtained for $\langle 6\rangle$ and $\langle 7\rangle$ 1D-LPSs, the APB energy with respect to $L1_2$ is slightly positive; the formation of APBs in the $L1_2$ structure to give 1D-LPSs of type $\langle M\rangle$ (M being an integer) is not energetically favoured. On the other hand, E'_{APB} is clearly positive: the creation of APBs in the $D0_{22}$ structure is not favourable energetically, and therefore the $D0_{22}$ structure is the stable one.

In the fully relaxed case, both E_{APB} and E'_{APB} are negative. Therefore, neither $L1_2$ nor $D0_{22}$ is the most stable structure, and indeed $D0_{23}$ is the ground state.

The values of E_{APB} and E'_{APB}, if they were obtained from the energy differences from $L1_2$ of $D0_{22}$ or of $D0_{23}$ structures, are reported in the two first rows of tables 4 and 5. Inspection of the values shows that, if the correct sign is almost always obtained, the values can differ by twice as much. Therefore, it is absolutely necessary to take into account the interactions between the APBs in order to obtain the APB energies. Moreover, it is necessary to perform *ab initio* calculations for a large number of 1D-LPSs to test the convergence of the expansion used in the APB model.

6.2. Constrained structures

Let us now consider the constrained 1D-LPSs. In this case, the values obtained for E_{APB} and E'_{APB} can be considered as those of isolated APBs either in $L1_2$ or in the $D0_{22}$ structures.

The values of $M(E_{\langle M\rangle}-E_{\langle\infty\rangle})$ obtained for the $\langle M\rangle$ 1D-LPSs constrained to have the same parameter as the equilibrium $L1_2$ structure are reported in figure 8. The values are practically constant from $M = 5$. The derived APB energies are reported in table 7.

The values of $M'(E_{\langle 21^j\rangle} - E_{\langle 1\rangle})$ obtained for the $\langle 21^j\rangle$ 1D-LPSs constrained to have the same parameter as the equilibrium $D0_{22}$ structure are reported in figure 9. As above, these values are practically constant from $M' = 5$. The derived APB energies are reported in table 8.

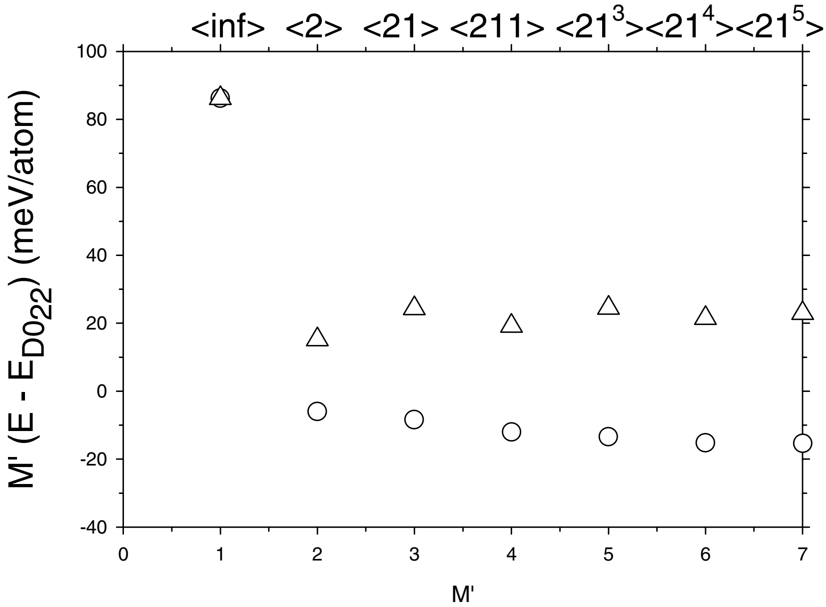

Figure 9. VASP-calculated values of the energy differences from $D0_{22}$ multiplied by M' of $\langle 21^j \rangle$ 1D-LPSs whose lattice parameter, a, has been constrained to that of the $D0_{22}$ structure. $\triangle$, distorted structures; $\bigcirc$, fully relaxed structures.

Table 7. APB energies with respect to $L1_2$ of the constrained $\langle M \rangle$ 1D-LPSs for the $L1_2$ lattice parameter a. The values are given in meV/atom.

	Distorted structures along z axis	Fully relaxed structures along z axis
$E_{D0_{22}} - E_{L1_2}$	33	33
$2(E_{D0_{23}} - E_{L1_2})$	4	−64
E_{APB} (method 1)	10	−42
γ_{APB} (mJ m^{-2})	40	170

Table 8. APB energies with respect to $D0_{22}$ for constrained 1D-LPSs at the lattice parameter a of the equilibrium $D0_{22}$ structure. The values are given in meV/atom.

	Distorted structures along z axis	Fully relaxed structures along z axis
$E_{L1_2} - E_{D0_{22}}$	86	86
$2(E_{D0_{23}} - E_{D0_{22}})$	30	−12
E_{APB} (method 1)	23	−15
γ_{APB} (mJ m^{-2})	98	65

As in section 6.1, we observe that the APB energies cannot be obtained solely from the energy differences from $L1_2$ of the $D0_{22}$ and $D0_{23}$ structures.

We must remark that method 2 indicated previously (section 6.1.2) has not been used because its application would necessitate the calculations of the $\langle 21^j \rangle$ energies at the $L1_2$

lattice parameter and $\langle M \rangle$ energies at the $D0_{22}$ lattice parameter to obtain the interaction coefficients with sufficient precision.

The values of the APB energies reported in tables 7 and 8 can be considered as the energy of an APB isolated either in the $L1_2$ or in the $D0_{22}$ structure. These values reported to the area unit are given by

$$\gamma/\mathrm{L1}_2 = \frac{E_{APB}}{a^2_{\mathrm{L1}_2}/4} \qquad \text{and} \qquad \gamma/\mathrm{D0}_{22} = \frac{E'_{APB}}{a^2_{\mathrm{D0}_{22}}/4}. \tag{7}$$

The factor of four has been introduced because the APB energies given in tables 7 and 8 are expressed per atom. a is the lattice parameter along x and y axes of either the $L1_2$ or the distorted $D0_{22}$ structure.

In the approach developed in section 6.1, we obtained the energetic parameters of an APB Ising model for the purpose of describing the behaviour of the $L1_2$, $D0_{22}$, $D0_{23}$ and other 1D-LPSs. In this section we have obtained the energy of an isolated APB. Although these approaches are different, the comparison of the APB energies obtained with the equilibrium 1D-LPSs and with the constrained ones indicates only small differences.

7. Summary and conclusions

Some years ago Paxton [17] showed that it is possible to bring together the theory of alloys, as seen from the density functional point of view, and practical problems in physical metallurgy. In the present work, we have employed such a strategy to obtain APB energies from *ab initio* calculations of cohesive energies. Indeed the cohesive energies of two series of 1D-LPSs, let us say $\langle M \rangle$ with M an integer and $\langle 21^j \rangle$, were obtained with a code based on the density functional theory in the GGA. The calculations were performed for rather large values of M or M' (up to M or $M' = 7$). More, these calculations were performed for ideal, distorted and fully relaxed structures. To improve the energy difference from $L1_2$ of the 1D-LPSs, $L1_2$ superstructures have been built and their cohesive energies calculated with the same number of k points as used for the corresponding 1D-LPS. The results have been discussed in the framework of an APB Ising model, whose parameters have been obtained. These calculations have shown that, in the case of ideal structures, APB formation is not energetically favoured in the $L1_2$ structure while it is energetically favoured in the $D0_{22}$ structure. In the distorted case, the APB energy is very small in the $L1_2$ structure, while it is strongly positive in the $D0_{22}$ structure. This supports the fact that $L1_2$ can be maintained in a metastable state and that $D0_{22}$ is the most stable structure at ordinary temperature. In the fully relaxed situation, which can be considered as the situation at very low temperature, the APB energies with respect to $L1_2$ and to $D0_{22}$ are both negative, showing that neither $L1_2$ nor $D0_{22}$ is the ground state; actually at $T = 0$ K the ground state is the $D0_{23}$ structure.

We have also proved, in this work concerning the $TiAl_3$ compound, that the energy differences from $L1_2$ of $D0_{22}$ and $D0_{23}$ structures solely are not sufficient to derive APB energies with a good precision. Moreover, we have also shown that, in the $TiAl_3$ compound, all the relaxation effects, cell-external distortion and cell-internal displacements of the atoms, must be taken into account in order to obtain correct values of the APB energies.

Finally we have shown that the energy of an isolated APB obtained with constrained 1D-LPSs is not very different from that obtained with the APB Ising model applied to the equilibrium 1D-LPSs.

References

[1] Sinha A K 1969 *Trans. AIME* **245** 911
[2] Johansson C H and Linde J O 1936 *Ann. Phys., NY* **25** 1
[3] Miida R, Kasahara M and Watanabe D 1980 *Japan. J. Appl. Phys.* **18** L707
[4] Loiseau A, Van Tendeloo G, Portier R and Ducastelle F 1985 *J. Physique* **46** 595
[5] Amador C, Hoyt J J, Chakoumakos B C and de Fontaine D 1995 *Phys. Rev. Lett.* **65** 4995
[6] Zhdanov G S 1945 *C. R. Acad. Sci. USSR* **48** 43
[7] Fisher M E and Selke W 1980 *Phys. Rev. Lett.* **44** 1502
[8] Fisher M E and Selke W 1981 *Phil. Trans. R. Soc.* **302** 1
[9] Bak P and Bruinsma R 1982 *Phys. Rev. Lett.* **49** 249
[10] Rosengaard N M and Skriver H L 1994 *Phys. Rev.* B **49** 14 666
[11] Kresse G and Furthmüller J 1996 *Phys. Rev.* B **54** 11 169
[12] Kresse G and Furthmüller J 1996 *Comput. Mater. Sci.* **6** 15
[13] Kresse G and Hafner J 1994 *J. Phys.: Condens. Matter* **6** 8245
[14] Perdew J P and Wang Y 1992 *Phys. Rev.* B **45** 13 244
[15] Villars P and Calvert L D 1985 *Pearson's Handbook of Crystallographic Data for Intermetallic Phases* (Materials Park, OH: American Society for Metals)
[16] Srinivasan S, Desch P B and Schwarz R B 1991 *Scr. Metall. Mater.* **25** 2513
[17] Paxton A T 1992 *Electron Theory in Alloy Design* ed D G Pettifor and A H Cottrell (The Institute of Materials) p 158